Nanoscale Advances

ROYAL SOCIETY OF CHEMISTRY

COMMUNICATION

View Article Online
View Journal | View Issue

Check for updates

Cite this: *Nanoscale Adv.*, 2020, **2**, 210

Received 14th October 2019
Accepted 16th December 2019

DOI: 10.1039/c9na00652d

rsc.li/nanoscale-advances

Photo/thermo-responsive and size-switchable nanoparticles for chemo-photothermal therapy against orthotopic breast cancer†

Ying Bi,‡[ab] Miao Wang,‡[ab] Lirong Peng,‡[a] Lifo Ruan,[bc] Mengxue Zhou,[bc] Yi Hu,*[bc] Jun Chen*[bc] and Jimin Gao*[a]

Tumor penetration of nanocarriers is still an unresolved challenge for effective drug delivery. Herein, we described a size-switchable nanoplatform in response to an external near-infrared (NIR) laser for transcellular drug delivery. The nanoplatform was constructed with a poly(*N*-isopropylacrylamide) (PNIPAM)-based nanogel encapsulating chitosan-coated single-walled carbon nanotubes, followed by loading a chemotherapeutic drug, doxorubicin (DOX). In mice bearing orthotopic breast tumors, the photothermal effect from single-walled carbon nanotubes upon NIR irradiation potently inhibited tumor growth. The antitumor effect of the nanomedicine with NIR irradiation might be attributed to its capability of transcellular transport and tumor penetration in mice. In addition, the nanomedicine with NIR irradiation could elicit an antitumor response by increasing cytotoxic T cells and decreasing myeloid-derived suppressor cells. These results validated the application of photo/thermo-responsive nanomedicine in the orthotopic model of breast cancer.

Despite the advances in developing nanocarriers for tumor-targeted drug delivery in the past decade, the translation of research results into clinics remains challenging.[1] One of the major hindrances is the insufficient penetration of nanocarriers in solid tumors.[2] Typically, nanocarriers can penetrate only a few cell layers post extravasation from the blood vessels.[2,3] Moreover, the uneven intratumoral distribution of delivered drugs may eventually result in compromised therapeutic efficacy regardless of treatment modalities.[4] To address the penetration issue, utilization of stimuli-responsive nanocarriers to overcome the complex physiological and pathological barriers is an intriguing strategy.[5,6] It is broadly acknowledged that the physicochemical characteristics, including size, surface charge and morphology, of nanoparticles substantially influence their tumor penetration and intracellular delivery.[7–10] Therefore, the nanocarriers with a size-switchable property upon tumor-confined stimuli will potentially enhance tumor penetration.

Photothermal therapy (PTT) by means of light-triggered heating through light-absorbing photothermal agents provides a spatiotemporally controllable tool for cancer treatment.[11] In addition to the direct ablation of tumor cells by light-induced hyperthermia, elevation of temperature can ameliorate the permeability of blood vessels inside tumors and boost the release of entrapped therapeutic payloads. For example, Kirui and co-workers have characterized how mild PTT could enhance the penetration of macromolecules in tumors.[12] Therefore, photothermal effects may act synergistically with size-switchable nanoparticles to enhance their tumor penetration ability.

Besides the suboptimal tumor penetration of nanocarriers, the deficiency of research in orthotopic tumor models might also impede the clinical translation of nanomedicines. The majority of preclinical studies of nanomedicines have exploited murine subcutaneous tumor models. However, these subcutaneous tumor models may not resemble the corresponding orthotopic tumor models in terms of vascular and stromal microenvironments.[13–15] Compared with subcutaneous tumor models, orthotopic tumor models generally better simulate the physiological situation and therefore can be a more reliable tool for evaluating the therapeutic effects of nanomedicines against cancers.[16] In particular, examination of tumor penetration of nanocarriers in orthotopic tumor models is necessary, as the tumor vasculature influences the tumor penetration of nanoparticles.[17,18]

We have developed a size-switchable nanocarrier in response to a near-infrared (NIR) laser for targeted drug delivery.[18–20] We used thermoresponsive poly(*N*-isopropylacrylamide) (PNIPAM) nanogels, which can shrink upon an increase in

[a]*Zhejiang Provincial Key Laboratory for Technology & Application of Model Organisms, School of Laboratory Medicine and Life Science, Wenzhou Medical University, Wenzhou, Zhejiang 325035, China. E-mail: jimingao64@163.com*

[b]*CAS Key Laboratory for Biomedical Effects of Nanomaterials and Nanosafety, Multidisciplinary Research Division, Institute of High Energy Physics, Chinese Academy of Sciences (CAS), Beijing 100049, China. E-mail: chenjun@ihep.ac.cn; huyi@ihep.ac.cn*

[c]*University of Chinese Academy of Sciences, Beijing 100049, China*

† Electronic supplementary information (ESI) available. See DOI: 10.1039/c9na00652d

‡ These authors contributed equally to this study.

temperature,[21,22] to encapsulate chitosan-wrapped carbon nanotubes as a NIR-responsive PTT agent.[23] When loaded with a chemotherapeutic agent doxorubicin (DOX), the nanoparticles have been shown to have potent antitumor activity in both subcutaneous and orthotopic mouse models of bladder cancer.[18,19] Herein, we aimed to further validate the antitumor effect of DOX-loaded nanoparticles (NP-DOX) in a mouse model of orthotopic breast cancer and examine the tumor penetration of nanoparticles upon NIR irradiation (Scheme 1). In addition, our data suggested that NP-DOX with NIR irradiation could elicit an antitumor immune response.

Results and discussion

The nanoparticles in this study were prepared according to a reported protocol.[19] One major component of the NPs, PNIPAM, features a thermoresponsive phase transition that might change the size of the NPs in response to the surrounding temperature. To demonstrate the thermoresponsive size change of NP-DOX, we measured the size of NP-DOX at different temperatures by dynamic light scattering (DLS). As shown in Fig. 1, when the temperature was increased from 37 °C to 42 °C, the hydrodynamic size of NP-DOX changed from ~320 nm to ~240 nm. Afterward, we decreased the temperature to 37 °C, and the size of NP-DOX was back to ~300 nm (Fig. 1). The size shrinkage of nanoparticles underwent little decay after three rounds of temperature changes, thereby suggesting that the nanoparticles were relatively stable.

At the cellular level, lysosomes of 4T1 cells incubated with the NPs for a predetermined time were stained with green-colored fluorescent LysoTracker and observed by confocal microscopy. Without NIR, the lysosomes were generally observed as green fluorescent dots (Fig. 2A). By contrast, after NIR irradiation, the green dot-like lysosomes in the cells were fused with the neighboring dots, indicating the destabilization of lysosomes (Fig. 2A). The destabilization of lysosomes, which could be ascribed to the NIR-induced photothermal effect, may facilitate lysosomal escape of the NPs.[24] Next, we asked whether DOX was able to pass through the neighboring cells. As seen in Fig. 2B, the red fluorescence of DOX indicated the uptake of NP-DOX in the cells. At the beginning, the cellular uptake of NP-DOX was similar with or without NIR (Fig. 2B and C). However, DOX fluorescence from NP-DOX + NIR irradiation was much stronger than that from NP-DOX in coverslip II (1.8 times) and III (2.7 times) (Fig. 2B and C). These results suggested that NIR irradiation enhanced the transcellular transport of DOX.

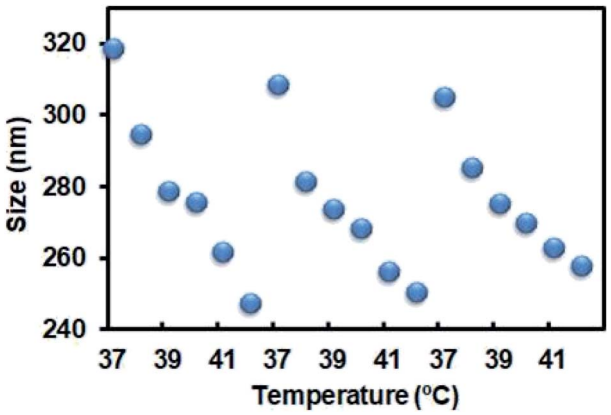

Fig. 1 Reversible size change behavior of NP-DOX at temperatures between 37 °C and 42 °C.

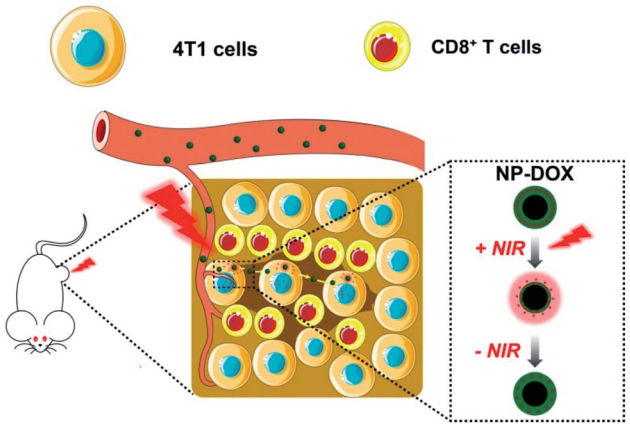

Scheme 1 Schematic illustration of NIR-responsive and size-switchable nanomedicines for chemo–photothermal therapy. This scheme uses elements from Servier Medical Art (https://www.smart.servier.com).

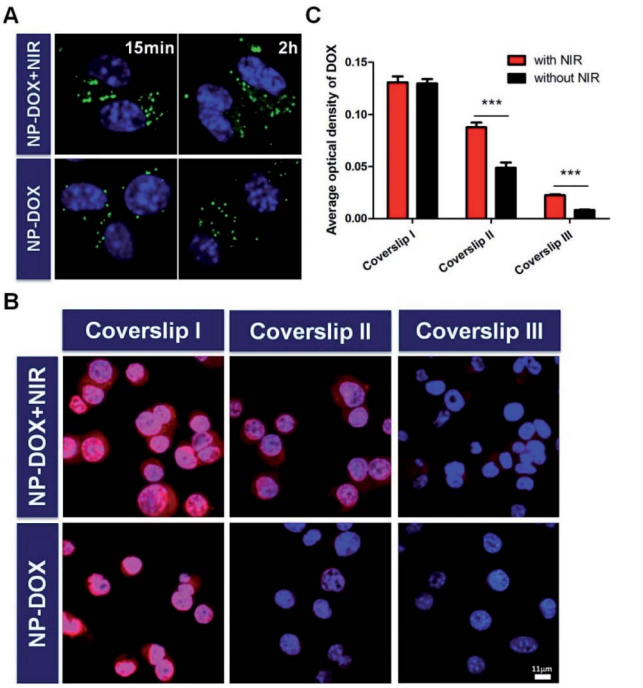

Fig. 2 (A) Lysosomes of 4T1 cells post incubation with NP-DOX with/without NIR irradiation for predetermined time were monitored by confocal microscopy. The lysosomes were stained with LysoTracker Green. (B) Successive transportation of DOX with/without NIR irradiation between 4T1 cells on three coverslips. The nuclei were stained with Hoechst 33342. (C) Quantitative analysis of DOX fluorescence in three sets of coverslips. ***, $P < 0.001$.

Encouraged by the excellent tumor-targeting and tumor penetration ability of NP-DOX with NIR irradiation, we proceeded to evaluate its antitumor activity in mice bearing orthotopic breast tumors. When the average sizes of tumors reached about 60 mm^3, the mice were administered with PBS, free DOX, NP-DOX, DOX plus NIR irradiation, NP plus NIR irradiation and NP-DOX plus NIR irradiation. Tumor volumes of the mice were recorded every three days. From the results of the tumor volumes, we found that NP and NP-DOX with NIR irradiation could potently inhibit tumor growth in mice (Fig. 3A and B). By contrast, the tumors continued to grow in mice upon the other four treatments (Fig. 3A and B). These results suggested that NIR-induced hyperthermia was able to suppress tumor growth. According to our previous report,[19] carbon nanotubes embedded in the nanocarriers could convert NIR efficiently into heat and consequently increase the tumor temperature to be higher than 50 °C. Such a high temperature prevented tumor growth. After the mice were sacrificed, the tumors from the NP-DOX + NIR group were significantly smaller than those from the NP + NIR group (Fig. 3C and D). These results suggested that there might be synergistic chemo–photothermal effects against tumors.

Hematoxylin and eosin (H&E) staining was employed to evaluate the antitumor efficacy of the nanoparticles. From H&E images (Fig. 4A), more apoptotic or necrotic cells were found in the NP-DOX plus NIR group in comparison to PBS and free DOX groups (Fig. 4B). Fig. 4C displays the results of the Ki-67 assay. With the aid of NIR irradiation, brown dots were reduced by NP-DOX (Fig. 4D), which indicated a potent inhibitory effect on tumor cell proliferation.

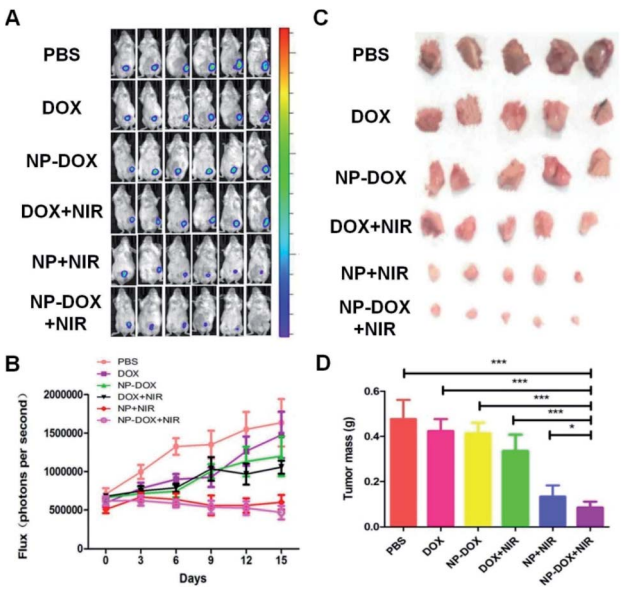

Fig. 3 (A) *In vivo* bioluminescence photographs to monitor the growth of Luc-4T1 orthotopic tumors. (B) Quantification of bioluminescence in mice. (C) Images of the tumors collected from different groups of mice at the end of the treatments. (D) Average weights of tumors collected from mice at the end of the treatments as indicated. *, $P < 0.05$; ***, $P < 0.001$.

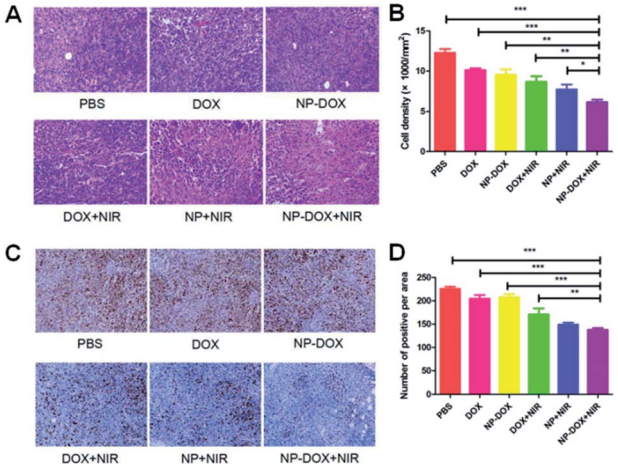

Fig. 4 (A) Typical H&E-staining images of tumor sections obtained from mice receiving the treatments as indicated. (B) Statistical data were obtained from 4 sections per tumor and 4 tumors per treatment group. (C) Typical immunohistology images of Ki-67-stained tumor slices from 24 h treatment mice after injections. (D) Statistical data were obtained from 4 sections per tumor and 4 tumors per treatment group. *, $P < 0.05$; **, $P < 0.01$; ***, $P < 0.001$.

Based on the superior therapeutic outcome of the photothermal and chemotherapy, we next asked whether the dying tumor cells might release a large amount of antigens and elicit local immune response.[25] In particular, tumor cells undergoing apoptosis could provide antigens for dendritic cells.[26] As professional antigen-presenting cells, dendritic cells play key roles in the initiation and regulation of anticancer immunity.[27] Therefore, we further studied the effects of NPs on dendritic cells. $CD11c^+$ dendritic cells are representative antigen-presenting cells for the induction of antitumor immunity.[28] We found that NP-DOX with NIR irradiation significantly increased the percentage of $CD11c^+$ dendritic cells, as compared with DOX and NP-DOX without NIR irradiation (Fig. S1A†). Similarly, NP-DOX with NIR irradiation significantly increased the percentage of $CD80^+CD86^+$ cells, as compared with DOX and NP-DOX without NIR irradiation (Fig. S1B†). These cells are mature dendritic cells which may induce a cytotoxic T cell response.[29] Based on these findings, we next tested the effects of DOX and NP-DOX on $CD8^+$ cells that are cytotoxic T cells combating cancer cells.[30] We found that NP-DOX with NIR irradiation also increased the percentage of $CD8^+$ cells (Fig. S2A†), while that of T helper cells $CD4^+$ remained almost unchanged (Fig. S2B†). NP-DOX/NIR-induced increase in $CD8^+$ cells was in agreement with the increase in $CD80^+CD86^+$ cells. Besides the anticancer immunity, we have also examined the negative regulator such as $CD4^+FoxP3^+$ cells, which are regulatory T cells (Tregs) and could be immunologic barriers for $CD8^+$ cells-mediated antitumor immune response.[30] Results indicated that the levels of $CD4^+FoxP3^+$ cells were similar between DOX, NP-DOX and NP-DOX with NIR irradiation (Fig. S3†). These results suggested that NP-DOX with NIR irradiation might not suppress $CD8^+$ cell-mediated antitumor immune response. Furthermore, we found that $CD11b^+Gr\text{-}1^+$ myeloid-derived suppressor cells were

significantly reduced by NP-DOX with NIR irradiation (Fig. S4†). As these cells have been suggested to be responsible for lung metastasis of breast cancer,[31] the NP-DOX/NIR-induced decrease in $CD11b^{+}Gr\text{-}1^{+}$ cells might prevent the tumor metastasis. These results provided preliminary data of NP-DOX/NIR-associated immune response. Further mechanistic studies would be required to elucidate how the immunologic system is activated by nanomedicines against cancer.

Conclusions

In summary, we have demonstrated that photo/thermo-responsive nanomedicines could provide synergistic chemo–photothermal therapy in mice bearing orthotopic breast tumors. The death of tumor cells upon NP-DOX and NIR might elicit $CD8^{+}$ cell-mediated antitumor immune response to further enhance the antitumor effects of NP-DOX. The findings in this study validated the application of photo/thermo-responsive nanomedicines in the orthotopic tumor model.

Conflicts of interest

There are no conflicts to declare.

Acknowledgements

This work was supported by the National Natural Science Foundation of China (21574136, 81573110, 11875269), the CAS Youth Innovation Promotion Association Program (2015008), Science Foundation of National Health Commission (WKJ-ZJ-1928), Science and Technology Major Projects of Wenzhou (ZJ2017014, 2018ZY001) and the Hundred Talents Program of CAS.

References

1 J. J. Shi, P. W. Kantoff, R. Wooster and O. C. Farokhzad, *Nat. Rev. Cancer*, 2017, **17**, 20–37.
2 R. Tong, H. D. Hemmati, R. Langer and D. S. Kohane, *J. Am. Chem. Soc.*, 2012, **134**, 8848–8855.
3 J. J. Chen, J. X. Ding, Y. C. Wang, J. J. Cheng, S. X. Ji, X. L. Zhuang and X. S. Chen, *Adv. Mater.*, 2017, **29**, 1701170.
4 H. Kobayashi, R. Watanabe and P. L. Choyke, *Theranostics*, 2014, **4**, 81–89.
5 M. X. Zhou, K. K. Wen, Y. Bi, H. R. Lu, J. Chen, Y. Hu and Z. F. Chai, *Curr. Top. Med. Chem.*, 2017, **17**, 2319–2334.
6 S. Mura, J. Nicolas and P. Couvreur, *Nat. Mater.*, 2013, **12**, 991–1003.
7 M. X. Zhou, H. Huang, D. Q. Wang, H. R. Lu, J. Chen, Z. F. Chai, S. Q. Yao and Y. Hu, *Nano Lett.*, 2019, **19**, 3671–3675.
8 P. Zhang, J. Wang, H. Chen, L. Zhao, B. Chen, C. Chu, H. Liu, Z. Qin, J. Liu, Y. Tan, X. Chen and G. Liu, *J. Am. Chem. Soc.*, 2018, **140**, 14980–14989.
9 K. K. Wen, M. X. Zhou, H. R. Lu, Y. Bi, L. F. Ruan, J. Chen and Y. Hu, *ACS Biomater. Sci. Eng.*, 2018, **4**, 4244–4254.
10 M. X. Zhou, X. C. Zhang, J. Xie, R. X. Qi, H. R. Lu, S. Leporatti, J. Chen and Y. Hu, *Nanomaterials*, 2018, **8**, 952.
11 Y. J. Liu, P. Bhattarai, Z. F. Dai and X. Y. Chen, *Chem. Soc. Rev.*, 2019, **48**, 2053–2108.
12 D. K. Kirui, E. J. Koay, X. J. Guo, V. Cristini, H. F. Shen and M. Ferrari, *Nanomedicine*, 2014, **10**, 1487–1496.
13 W. Zhang, W. Fan, S. Rachagani, Z. Zhou, S. M. Lele, S. K. Batra and J. C. Garrison, *Sci. Rep.*, 2019, **9**, 11117.
14 A. S. Fung, C. Lee, M. Yu and I. F. Tannock, *BMC Cancer*, 2015, **15**, 112.
15 E. Chan, A. Patel, W. Heston and W. Larchian, *BJU Int.*, 2009, **104**, 1286–1291.
16 J. J. Killion, R. Radinsky and I. J. Fidler, *Cancer Metastasis Rev.*, 1998, **17**, 279–284.
17 W. Shi, Y. X. Yin, Y. Wang, B. Zhang, P. Tan, T. Jiang, H. Mei, J. Deng, H. F. Wang, T. Guo, Z. Q. Pang and Y. Hu, *Oncotarget*, 2017, **8**, 32212–32227.
18 H. Gao, Y. Bi, X. Wang, M. Wang, M. X. Zhou, H. R. Lu, J. M. Gao, J. Chen and Y. Hu, *ACS Biomater. Sci. Eng.*, 2017, **3**, 3628–3634.
19 H. Gao, Y. Bi, J. Chen, L. R. Peng, K. K. Wen, P. Ji, W. F. Ren, X. Q. Li, N. Zhang, J. M. Gao, Z. F. Chai and Y. Hu, *ACS Appl. Mater. Interfaces*, 2016, **8**, 15103–15112.
20 Y. P. Qin, J. Chen, Y. Bi, X. H. Xu, H. Zhou, J. M. Gao, Y. Hu, Y. L. Zhao and Z. F. Chai, *Acta Biomater.*, 2015, **17**, 201–209.
21 D. Q. Wang, H. Huang, M. X. Zhou, H. R. Lu, J. Chen, Y. T. Chang, J. M. Gao, Z. F. Chai and Y. Hu, *Chem. Commun.*, 2019, **55**, 4051–4054.
22 D. Wang, M. Zhou, H. Huang, L. Ruan, H. Lu, J. Zhang, J. Chen, J. Gao, Z. Chai and Y. Hu, *ACS Appl. Bio Mater.*, 2019, **2**, 3178–3182.
23 Y. Liu, H. P. Li, J. Xie, M. X. Zhou, H. Huang, H. R. Lu, Z. F. Chai, J. Chen and Y. Hu, *Biomater. Sci.*, 2017, **5**, 1022–1031.
24 X. Yang, B. Fan, W. Gao, L. Li, T. Li, J. Sun, X. Peng, X. Li, Z. Wang, B. Wang, R. Zhang and J. Xie, *Int. J. Nanomed.*, 2018, **13**, 4333–4344.
25 A. Balasubramani, *Science*, 2019, **364**, 1247.
26 M. L. Albert, *Nat. Rev. Immunol.*, 2004, **4**, 223–231.
27 P. Giovanelli, T. A. Sandoval and J. R. Cubillos-Ruiz, *Trends Immunol.*, 2019, **40**, 699–718.
28 H. Lee, H. J. Lee, I. H. Song, W. S. Bang, S. H. Heo, G. Gong and I. A. Park, *In Vivo*, 2018, **32**, 1561–1569.
29 J. Lee, S. N. Sait and M. Wetzler, *Int. Immunol.*, 2004, **16**, 1377–1389.
30 B. Farhood, M. Najafi and K. Mortezaee, *J. Cell. Physiol.*, 2019, **234**, 8509–8521.
31 Y. L. Hsu, M. C. Yen, W. A. Chang, P. H. Tsai, Y. C. Pan, S. H. Liao and P. L. Kuo, *Breast Cancer Res.*, 2019, **21**, 23.